

## **A Comparative study on structural and magnetic properties of La, Cr and Al doped M-type Calcium hexagonal nano ferrites prepared by Sol gel auto-combustion method**

B.S.Satone<sup>1</sup>, K.G.Rewatkar<sup>2</sup>,

<sup>1</sup> Department of Physics, S.H.J.C., Nagpur

<sup>2</sup> Department of Physics, Dr. Ambedkar college, Nagpur.

**Abstract-**Nano particles of Calcium substituted ferrites namely  $\text{CaLa}_1\text{Fe}_{11}\text{O}_{19}$ ,  $\text{CaCr}_1\text{Fe}_{11}\text{O}_{19}$  and  $\text{CaAl}_1\text{Fe}_{11}\text{O}_{19}$  have been chosen for their comparative studies on structural and magnetic properties. Above ferrite samples were successfully synthesized by sol gel auto combustion method. X-ray diffraction studies revealed the formation of mono phase M type hexagonal ferrite with mono phase space group  $P6_3/mmc$  (no194). The SEM and TEM were studied, which confirmed that the sample exhibit relatively well defined hexagonal like grains with average particle size in the range 52 nm to 38nm. The values of the lattice parameters supports this conformation.

The magnetic measurements were carried by using Vibration Sample Magnetometer (VSM) shown that, as compared to La and Cr, the Al doped sample leads to a increase in saturation magnetization and to a significant increase in the coercive field. Thus the magnetic characters of the Al doped samples are superior than that of La and Cr doped calcium hexaferrites. It is known that the nano-hexaferrites with such special magnetic properties are highly useful in Data storage applications.

**Keywords:** Nano ferrite, Sol-gel Auto-combustion, XRD, TEM, VSM, etc.

### **I. INTRODUCTION**

Ferrites are one of the most widely used electromagnetic material for a broad category of applications over a wide frequency range due to their low cost and high performance [1]. Recently researches on ferrites have been shifted on nanoferrite material as the size of the particle is smaller than the critical size, the particles exhibit single domain state and domain wall resonance is avoided [2,3], due to this, material can work at higher frequency [4].

The Hexagonal ferrites show good chemical and thermal stability which would result in longer storage life of the media. These have been used in bulk form for many applications due to their hard magnetic properties, for example, as permanent magnets. In the recent years, these ferrites have drawn a great interest for magnetic recording media [5,6]. Hexagonal ferrites are known for their strong uniaxial magneto crystalline anisotropy with ease of magnetization along c-axis [7]. Most substitutions in hexagonal ferrites reduce the anisotropy field to obtain hysteresis properties suitable for various applications [8 -10].

The nanosized ferrite particles can be produced by a large numbers of methods like co-precipitation of hydroxides, sol gel synthesis, hydrothermal synthesis [11, 12] etc. In the present paper we have reported the results of powder formed by sol gel auto combustion method as this route provides a good control over the particle size and produce samples in relatively short time.

There are many reports where  $\text{Fe}^{3+}$  ion has been replaced in Ba/Sr hexagonal ferrites by different combination of substitution like trivalent cations viz.  $\text{Mn}^{3+}$ ,  $\text{Ga}^{3+}$ ,  $\text{Gd}^{3+}$ ,  $\text{Co}^{3+}$  [13,14]. or by the combination of divalent - tetravalent like  $\text{Zn}^{2+}$ - $\text{Ti}^{4+}$ ,  $\text{Co}^{2+}$ - $\text{Ti}^{4+}$ ,  $\text{Co}^{2+}$  -  $\text{Ir}^{4+}$ ,  $\text{Zn}^{2+}$ -  $\text{Sn}^{4+}$ ,  $\text{Co}^{2+}$ - $\text{Zr}^{4+}$  [15 – 19]. It has been observed that the Calcium Hexaferrites remain less attempted, hence in this

communication, we are reporting synthesis of  $\text{La}^{3+}$ ,  $\text{Cr}^{3+}$  and  $\text{Al}^{3+}$  ions substituted calcium hexaferrites and to study its structural and magnetic properties.

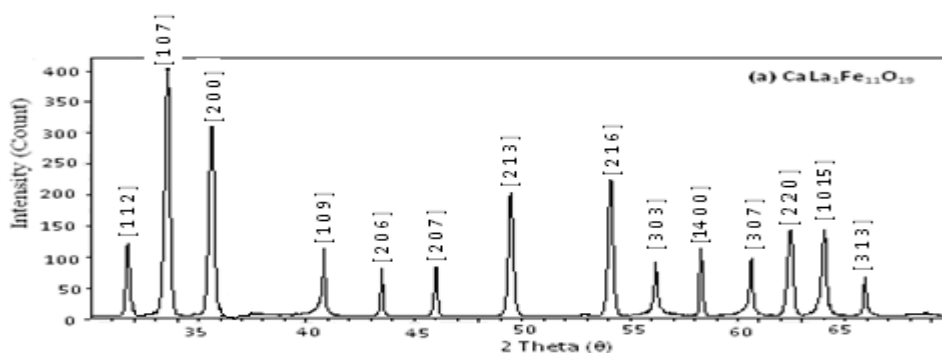
## II. EXPERIMENTAL

The samples of M-type substituted hexaferrites with formulae  $\text{CaLa}_1\text{Fe}_{11}\text{O}_{19}$ ,  $\text{CaCr}_1\text{Fe}_{11}\text{O}_{19}$  and  $\text{CaAl}_1\text{Fe}_{11}\text{O}_{19}$  were synthesized by sol gel auto-combustion method. The reactive nitrates such as  $\text{Ca}(\text{NO}_3)_2 \cdot 4\text{H}_2\text{O}$ ,  $\text{Fe}(\text{NO}_3)_3 \cdot 9\text{H}_2\text{O}$ ,  $\text{La}(\text{NO}_3)_3 \cdot 9\text{H}_2\text{O}$  /  $\text{Cr}(\text{NO}_3)_3 \cdot 9\text{H}_2\text{O}$  /  $\text{Al}(\text{NO}_3)_3 \cdot 9\text{H}_2\text{O}$  were dissolved into an unionized distilled water and heated at the temperature of  $60^\circ\text{C}$  for about 3 h with urea used as fuel, which gives requisite energy to initiate exothermic reaction. This gel was then kept in digitally controlled microwave oven and was fired to obtain the fine powder (ash) of samples. The ash was then collected and grinded for 5 hours in pestal mortar to get ultra-fine homogeneous powder of samples. The sample was then heated in electric furnace up to  $800^\circ\text{C}$  for about 8 h by increasing the temperature slowly ( $100^\circ\text{C}/\text{h}$ ) and then cooled at the same rate. Finally the sample was again grinded in pestal mortar for about an hour. The samples so produced are then kept in humidity free atmosphere in air tight container.

The phase structure of hexaferrite powders were investigated by (Philips diffractometer PW 3710) X ray diffraction Cu-K $\alpha$  radiation ( $\lambda = 1.54060\text{\AA}$ ). The Phase identification was executed using a X powder software and X-ray diffractograms were also plotted with X-Powder software. The structure morphology was identified using SEM instrument Cameca SU – SEM Probe and the TEM studies of prepared samples were done by using TEM Model Philips CM – 200. The magnetic parameters were measured with 14 T model, with a maximum field of 20 kOe. Characterization is focused on mainly three parts:(i) Saturation magnetization ( $M_s$ ), (ii) Coercive force or coercivity ( $H_c$ ), and (iii) Remanence magnetization ( $M_r$ ).

## III. RESULTS & DISCUSSION:

The XRD patterns of the investigated ferrite samples (Fig. 1) show characteristic diffraction peaks corresponding to the M-type barium ferrite structure. Absence of secondary peaks in XRD pattern gives the evidence of purely crystallized single phase [20] hexagonal M-structure pertaining to space group (SG: $P6_3/mmc$ ) (no194) which confirms that phase belongs to Magnetoplumbite [21], indicating that the crystal structure does not transform and remains single phase hexagonal magnetoplumbite after substitution with  $\text{La}^{3+}$ ,  $\text{Cr}^{3+}$ ,  $\text{Al}^{3+}$  ions respectively. The recorded values of lattice parameters also strengthen the results, as the values lie within the lattice parameter range ( $a = 5.8\text{--}5.9\text{\AA}$  and  $c = 22\text{--}23\text{\AA}$ ) of pure magnetoplumbite phase of hexaferrites. Moreover, the intensity of the peaks becomes stronger and narrower, indicating a better structural quality of materials [22]. The average particle size  $D$  of synthesized compounds were calculated from the broadening of the respective high intensity peak using the Scherer's equation [23]. It shows the particle size of ferrites were in the range 52 – 38 nm, which was also confirmed by SEM (fig 2) and TEM studies.(fig3).



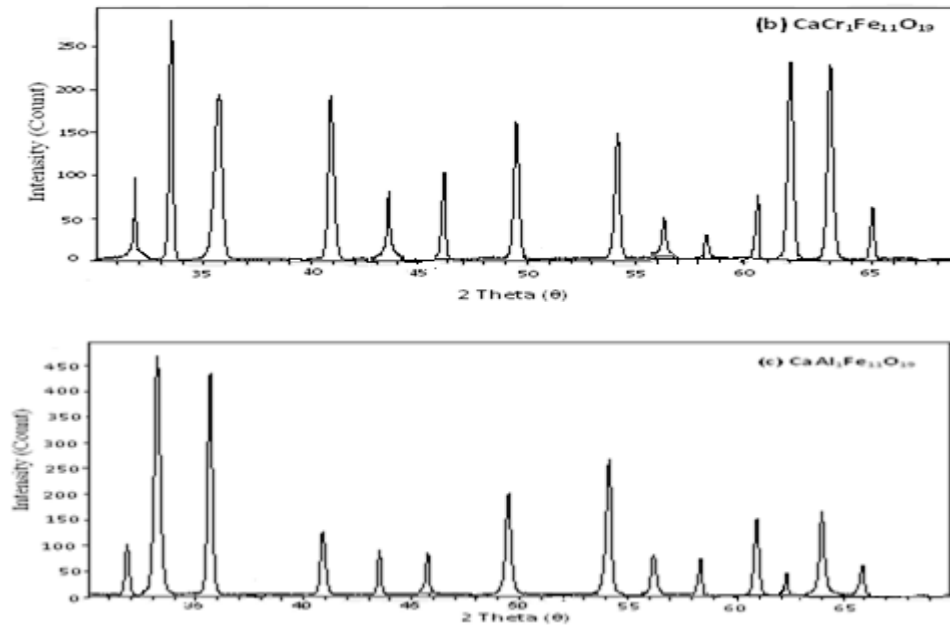


Fig.(1): XRD Pattern of synthesized Ca Substituted Hexaferrite

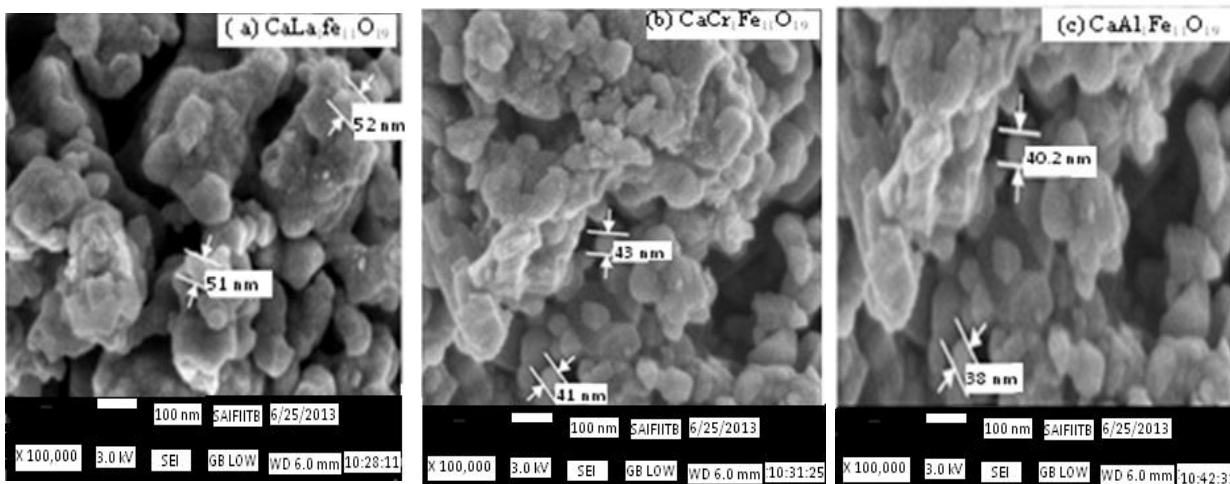


Fig (2): SEM Micrographs of Synthesized compounds

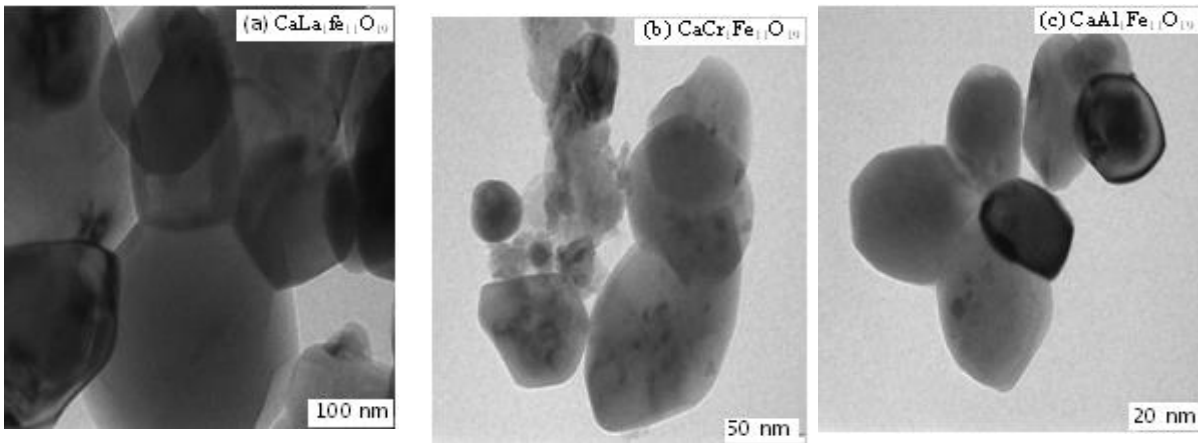


Fig (3): TEM Micrographs of Synthesized compounds

The average particle size, lattice parameters, X-ray density, bulk density, and porosity were calculated for each sample and are listed in Table 1. The variations of lattice parameters (a, c) shown in Table 1. can be attributed to substituted cations as the ratio of c/a has remained fairly constant [24]. It can also be explained on the basis of ionic radii. It is evident that the lattice parameters are smaller for the content  $Al^{3+}$  as compared to contents  $Cr^{3+}$  and  $La^{3+}$  respectively. This is due to relatively small ionic radius of  $Al^{3+}$  (0.53 Å) compared to that of  $Cr^{3+}$  (0.62 Å) and  $La^{3+}$  (1.03 Å) respectively. Similar behavior was reported for Co-Al substituted calcium ferrite by Ounnunkad [25] and Rewatkar et al. [26] and for Aluminium substituted Calcium Hexaferrites by Sanjay R. Gawali et al. [27]. Due to relatively small lattice constant and particle size interaction and solubility between  $Fe^{3+}$  ion and  $Al^{3+}$  ion is higher than other trivalent ions in the investigated compounds.

The variation in the densities shows general behavior that is the actual (experimental) density d values were found to be in general less than those of X-ray density  $d_x$  (theoretical density) which are expected due to presence of unavoidable pores created during firing [28]. During firing oxygen ions diffuse through the material on which densification of samples depends. The variation in porosity attributes to function of lattice parameters; it is reported that if densification increases, the volume of unit cell and lattice constant ultimately decrease and vice-versa [29, 30], this is in good agreement with our results.

Table 1: structural data

S.No.	sample	Lattice parameters		Axial ratio c/a	Cell vol. ( $\text{\AA}^3$ )	Bulk density, d ( $\text{gm/cm}^3$ )	X-ray density, $d_x$ ( $\text{gm/cm}^3$ )	Porosity %	Particle size D nm
		a ( $\text{\AA}$ )	c ( $\text{\AA}$ )						
1	CaLa <sub>1</sub> Fe <sub>11</sub> O <sub>19</sub>	5.8190	22.122	3.80	647.55	2.0429	5.6237	63	52
2	CaCr <sub>1</sub> Fe <sub>11</sub> O <sub>19</sub>	5.8147	22.115	3.80	647.15	2.6201	5.0505	48	43
3	CaAl <sub>1</sub> Fe <sub>11</sub> O <sub>19</sub>	5.8112	22.098	3.80	646.67	3.3529	5.1881	35	38

In the present work, the magnetic measurements for all the samples  $\text{CaLa}_1\text{Fe}_{11}\text{O}_{19}$ ,  $\text{CaCr}_1\text{Fe}_{11}\text{O}_{19}$  and  $\text{CaAl}_1\text{Fe}_{11}\text{O}_{19}$  have been carried out by using high field hysteresis loop technique at room temperature and the data obtained were tabulated in Table 2. Typical hysteresis loops of the samples are shown in Fig.4. In M-ferrites  $\text{Fe}^{3+}$  ions occupy five crystallographic sites three of which are octahedral (2a, 12k and 4f<sub>2</sub>), one tetrahedral (4f<sub>1</sub>) and one trigonal bipyramidal (2b) by Gorter (1954) [31]. Further it has been found that 12k, 2a and 2b have their spins in upward direction, 4f<sub>1</sub> and 4f<sub>2</sub> have downward spin and the resulting magnetic moment of  $\text{MFe}_{12}\text{O}_{19}$  (M = Ca, Sr, Ba and Pb) is due to the upward spins [32].

**Table 2: Variation of magnetic properties of synthesized calcium hexaferrites with substitutions of La, Cr and Al**

S. No	Name of sample	Ms (emu/g) $10^{-3}$	Mr (emu/g) $10^{-3}$	Hc (Gauss)	SQR ratio Mr/Ms
1	$\text{CaLa}_1\text{Fe}_{11}\text{O}_{19}$	99.524	14.703	192.85	0.15
2	$\text{CaCr}_1\text{Fe}_{11}\text{O}_{19}$	14.804	3.1922	1045.0	0.21
3	$\text{CaAl}_1\text{Fe}_{11}\text{O}_{19}$	67.7653	28.009	3386.1	0.41

Table 2 shows the variation of magnetic properties of parent calcium hexaferrite with substitution of La, Cr and Al. The saturation magnetization decreases with the substitution of La, Al and Cr, which decreases from  $99.524 \times 10^{-3}$  emu for La to  $14.804 \times 10^{-3}$  emu for Cr as observed from Table 2. The low value of saturation magnetization (Ms) owing to the magnetic moments of ions are not able to cancel out with spin down moments of  $\text{Fe}^{3+}$  ions ( $5 \mu\text{B}$ ). This is further related to low magnetic moment of  $\text{Cr}^{3+}$  ions ( $3 \mu\text{B}$ ) [33]. The decrease in the value of Ms due to the doping of  $\text{Cr}^{3+}$  ions in CaM can be explained on the basis, that the  $\text{Fe}^{3+}$  (magnetic moment  $5 \mu\text{B}$ ) are replaced by lesser magnetic  $\text{Cr}^{3+}$  ions (magnetic moment  $3 \mu\text{B}$ ) in the octahedral (B) sites of the ferrite sublattice, which causes weakening of super-exchange interaction of type  $\text{Fe}_A^{3+}-\text{O}-\text{Fe}_B^{3+}$ , leading to collapse of magnetic co-linearity of the lattice [34].

The increase in Saturation magnetization with non magnetic  $\text{Al}^{3+}$  ions substitution as compared to  $\text{Cr}^{3+}$  ions substitution can be explained on the basis that there is no opposition to the magnetic moment of  $\text{Fe}^{3+}$  ions ( $5 \mu\text{B}$ ) by  $\text{Al}^{3+}$  ( $0 \mu\text{B}$ ) ions. During the replacement of  $\text{Fe}^{3+}$  ( $5 \mu\text{B}$ ) ions by  $\text{Al}^{3+}$  ( $0 \mu\text{B}$ ) ions, 85% of Al ions occupies Octahedral and 15% occupies tetrahedral sites. Thus substitution of non magnetic  $\text{Al}^{3+}$  decreases  $\text{Fe}^{3+}$  ion concentration in both the sites causing magnetization reduction [35] and from our observations reduction in case of Al is less as compared to Cr. Similar variations of the saturation magnetization, remanence have also been reported for  $\text{Al}^{3+}$  and  $\text{Cr}^{3+}$  doped barium hexaferrite samples by Fang *et al.* (2005) [36], Singhal *et al.* (2005) [37] and Ounnunkad *et al.* (2006) [38]. The enhancement in saturation magnetization with La substitution can be explained on the basis of the characteristics of the distribution non-magnetic  $\text{La}^{3+}$  ions in the sublattice sites. If  $\text{La}^{3+}$  ions enter 4f<sub>1</sub> (tetrahedral) and 4f<sub>2</sub> (spin down) sites more than they enter 12k, 2a and 2b sites (spin up), net magnetic moment will increase [39].

The usefulness of a particular magnetic material for a specific application depends on its relevant properties. One of the property is the coercivity of the M-type hexaferrites. High coercivity is the demand of a hard magnet while low coercivity is the need of a soft magnet. The former is needed for energy storage applications. The later is needed for information storage recording media [40]. The steep fall in coercivity indicates conversion of hard ferrite into soft ferrite. Thus  $\text{CaAl}_1\text{Fe}_{11}\text{O}_{19}$  assumes more hard ferrite in nature than that of  $\text{CaLa}_1\text{Fe}_{11}\text{O}_{19}$  Ferrite.

There is an increase in coercivity value with  $\text{Al}^{3+}$  ions (diamagnetic) substitution for  $\text{Fe}^{3+}$  ions, which may be due to increase in magnetic anisotropy [41]. In the  $\text{Al}^{3+}$  doped  $\text{CaAl}_1\text{Fe}_{11}\text{O}_{19}$  sample high coercivity 3386 G is observed, which may be due to uniaxial magneto crystalline anisotropy along c-axis. There is remarkable fall in coercivity with the substitution of  $\text{La}^{3+}$  ions (192.85 G). The replacement of  $\text{Fe}^{3+}$  ions by substituted ions at 12k and 2b sites underlies the fast reduction in coercivity. These two sites contribute to a large anisotropy field, Mendoza-Surez [42]. The lowest value of coercivity for the  $\text{La}^{3+}$  ion doped samples  $\text{CaLa}_1\text{Fe}_{11}\text{O}_{19}$  may be due to the replacement of iron ions from 12k site to results in a reduction in the magneto-crystalline anisotropy. This consequently decreases the coercivity for the samples of  $\text{CaLa}_1\text{Fe}_{11}\text{O}_{19}$  hexaferrite. Similar type of variations have reported by Fang *et al.* (2005) [36], Singhal *et al.* (2005) [37] and Ounnunkad *et al.* (2006) [38].

The second effect accompanying reduction in coercivity is extrinsic, causing increase in grain size with substitution. Similar behavior is observed in TEM microstructure shown in Fig.2, this resembles with literature report given by Dho (2005) [43] about inverse nature of coercivity with grain size. Large number of inter granular pores are observed in Calcium Lanthanum ferrite, which decreases with substitution. The pores act as non-magnetic inclusions and discourage grain connectivity. The decrease in strength of these pores corresponds with increase in grain size, thereby decreasing coercivity. It also reaffirms that porosity strongly affects coercivity.

The lowest value of coercivity for  $\text{CaLa}_1\text{Fe}_{11}\text{O}_{19}$  may be due to the fact that a part of the particles in the sample do not have a perfect hexagonal shape, so that structural defects exist, which may also cause the reduction in the sample coercivity. Kubo *et al.* (1985)[44] investigated the particles shape effect on the coercivity of hexaferrites. They found that  $H_c$  decreased with increasing critical diameter 'D' for single domain / thickness  $t$ . On the other hand, Chang *et al.* (1993) [45] showed that incoherent reversal was occurring in the single domain extremely dependent on the thickness of the particles. Thus, it is believed that the lower coercivity may be caused not only by the larger aspect ratio, but also by an incoherent magnetization reversal.

The values of SQR (squareness ratio i.e.  $M_r/M_s$ ) are essentially a measure of squareness of the hysteresis loop. The squareness (SQR) should be less than 0.5 for the single domain magnetic structure of the sample. In our case, all the sample have SQR is less than 0.5 (Table 2) which eventually confirms the single domain structure for the samples [46]. In general, large SQR values (in the region of 0.5) are preferred in many applications such as recording media. It is known that the nano-hexaferrites with such special magnetic properties are highly useful in Data storage applications [47,48]. In the present investigation, the sample  $\text{CaAl}_1\text{Fe}_{11}\text{O}_{19}$  has high value of SQR. Hence it can be the promising material for recording media application.

#### IV. CONCLUSION

The samples of Lanthanum, Chromium and Aluminium doped calcium hexaferrites were successfully synthesized by the microwave induced sol-gel auto combustion method. The XRD analysis confirms the formation of mono phase M-type hexagonal ferrite. The values of the lattice parameters supports this Conformation. The space group of synthesized samples is found to be  $P6_3/mmc$ . (No. 194). The SEM and TEM study confirmed that samples exhibit relatively well defined, hexagonal like grains with average size in the range 52 nm to 32 nm.

The reduction of particle size of hexaferrites samples to nano range greatly improves the magnetic properties such as saturation magnetization, remanent magnetization and coercivity. The particle size of Al doped sample is small as compared to La and Cr doped samples. It was found that doping of Al in CaM as compared to La and Cr leads to a increase in saturation magnetization and to a significant increase in the coercive field due to the increase of magnetic anisotropy field. The magnetic characters

of the Al doped samples are observed to be of immense vital improvisation. Thus, the Al substituted calcium hexaferrites have superior magnetic properties than that of La and Cr substituted.

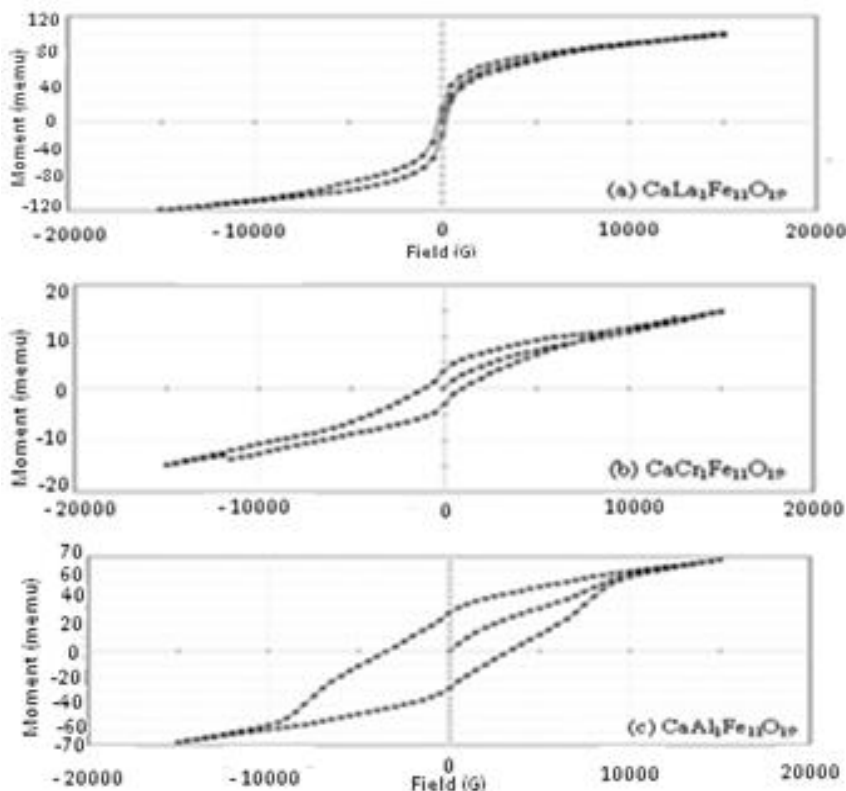


Fig.(4): Hysteresis loops for samples of synthesized Ca substituted hexaferrite of (a) CaLa<sub>1</sub>Fe<sub>11</sub>O<sub>19</sub> (b) CaCr<sub>1</sub>Fe<sub>11</sub>O<sub>19</sub> (c) CaAl<sub>1</sub>Fe<sub>11</sub>O<sub>19</sub>

## REFERENCES

- [1] J. Wang, P. F. Chong, S. C. Ng, L. M. Gan., *Mater.Lett.*30, 217, (1997).
- [2] M. Grigorova, H. J. Blythe, V. Balaskov, V. Rusnov, V. Masheva, D. Nihtianova, L .H. Martinez, J. S. Munoz, M. Mikhov., *J. Magn. magn Mater.* 183, 163, (1988).
- [3] J. Smith, H. P. J. Vijn., *Ferrites Philips Technical Library, Eindhoven* 73,(1959).
- [4] B. Parvatheeswara Rao, O. F. Caltun., *J. optoelectronics and advanced materials* .8, 991, (2006).
- [5] D. E. Speliotis., *IEEE Trans. Magn.* 25, 4048,(1989).
- [6] R. G. Simmons., *IEEE Trans. Magn.* 25, 4051 (1989).
- [7] S. Kanagesan, S. Jesurani, R. Velmurugan, S. Prabu, T. Kalaivani., *J. Mater. Sci., Mater. Electron.* 23, 1127,(2012).
- [8] P. Wartewig, M. K. Krause, P. Esquinazi, S. Roesler, R. Sonntag., *J Magn Magn Mater* 192,83,(1999).
- [9] O. Kubo, E. Ogawa., *J Magn. Magn. Mater.* 134,376,( 1994).
- [10] Z.W. Li, L. Chen, C. K. Ong., *J Appl Phys*, 92,3902,(2002).
- [11] S. R. Gavali, K. G. Rewatkar, V. M. Nanoti., *Advances in applied science research*, 3,2672,( 2012).
- [12] L.E.Smart, E.A. Moore., *Solid state Chemistry –an introduction-Third Edition-* (2005).
- [13] S. A. Masti., *J. Eng.ineering, Computers & Applied Sciences (ISSN No: 2319-5606)* , 2,12,(2013).
- [14] P. R. Moharkar, S. R. Gawali, K.G. Rewatkar, S.N. Sable and V.M.Nanoti., *Int. J. Knowledge Engineering (ISSN: 0976-5816 & E-ISSN: 0976-5824)*, 3, 113,( 2012).
- [15] C.S Wang, F.L Wei, M Lu, D.H Han, Z Yang., *J. Magn. magn Mater.* 183,241,(1998).
- [16] C. Singh , S. B. Narang , I.S. Hudiara , Y. Baib, K. Marina., *Mat. Lett.* 63,1921, (2009).
- [17] M. N. Giriya, C. L. Khobaragade, K. G. Rewatkar, R.P. Tandon., *Int. J. Scientific & Eng. Research*, (ISSN 2229-5518), 3, 10,(2012).
- [18] C.K Ong, H.C Fang , Z Yang, Y Li, *J. Magn. magn Mater.* 213,413,(2000).

- [19] A. Deshpande, S. N. Sable, V. M. Nanoti, K. G. Rewatkar., *Int. J. Knowledge Eng. (ISSN: 0976-5816 & E-ISSN) 3, 140, (2012).*
- [20] R. H. Kadam, A. Karim, A. B Kadam, A.S. Gaikwad and S. E. Shirsath., *Int. nanoletters 2,28,(2012).*
- [21] S. R. Gawali, K. G. Rewatkar, V. M. Nanoti., *Adv. in Appl. Sc. Res., 3, 2672, (2012).*
- [22] S. N. Sable, K. G. Rewatkar, V.M. Nanoti ., *Int.J. Mat. Sc. Eng. 168, 156, (2010).*
- [23] B.E. Warren, *X-Ray Diffraction, (Addison-Wesley, Reading, Massachusetts, 1969).*
- [24] R. K. Mahadule, P. R. Arjunwadkar, and M. P., *Int. J. Metals (Article ID 1989700), 10,1155,(2013).*
- [25] S. Ounnunkad , P. Winotai , *J. Magn. Magn. Mater. 301, 292,( 2006).*
- [26] K. G. Rewatkar, N. M. Patil, S. R.Gawali., *Bull. Mater. Sci. 28, 585,( 2005).*
- [27] S. R. Gawali, K. G. Rewatkar and V. M. Nanoti., *Adv. Appl. Sci. Res., 3,2672,(2012).*
- [28] A. Deshpande, S. N. Sable ,V. M. Nanoti ,K. G. Rewatkar., *Int. J. Knowledge Eng., 3,140,(2012).*
- [29] K. G. Rewatkar, N. M. Patil, S. Jaykumar, D. S. Bhowmick, M. N. Giriya., *J. Magn. Magn. Mat. 316,19,(2007).*
- [30] D. Seifert, J. Töpfer, F. Langenhorst, J. M. Le Breton, H. Chiron., *J. Magn.Magn.Mat.,321,4045,(2009).*
- [31] E. W. Gorter., *Proc. JEE 1048,255, (1957).*
- [32] L G Van Uitert, *J. Appl. Phys. 28, 317,(1957).*
- [33] S. A. Masti, A. K. Sharmab, P. N. Vasambekar., *Int. J. Science, Eng. and Tech. Research 3,3,(2014).*
- [34] M. Raghasudha, D. Ravinder, and P. Veerasomaiah., *J. Chem., (Article ID 804042), 10,1155,(2013).*
- [35] Suman and N. D. Sharma., *Indian J. pure and Applied Phsics, 45,551,(2007).*
- [36] Q. Q., Fang, H. Cheng, K. Huang, J.Wang., R. Li, Y.Jiao., *J. Magn. Magn. Mater. 294,281, (2005).*
- [37] S. Singhal , A. N. Garg , K. Chandra , *J. Magn. Magn. Mater. 285, 193, (2005).*
- [38] S. Ounnunkad , P. Winotai , *J. Magn. Magn. Mater. 301, 292,(2006).*
- [39] T. T. V. Nga, T. D. Hien, N. P. Duong and T. D. Hoang., *J. the Korean Physical Society, 52,1474,(2008).*
- [40] S. R. Gawali, P. R. Mohorkar, S. N. Sable, V.M. Nanoti, K. G. Rewatkar., *Int. J. Knowledge Engineering (ISSN: 0976-5816 & E-ISSN: 0976-5824) 3,25, (2012).*
- [41] S. Singhal , T. Namgyal , J.m Singh , K. Chandra , S. Bansal., *Ceramics International 37,1833, (2011).*
- [42] G. Mendoza-Surez, L. Rivas-VAzquez, J. Corral-Huacuz, A. Fuentes., *J. Escalante-Garcia, Physica B, 339, 110, (2003).*
- [43] J. Dho, K Lee, J Park, N Hur, *J Magn Magn Mater, 285, 164, (2005).*
- [44] P. Brissonneau, *J. Phys. Chem. Solids 7, 22, (1958).*
- [45] J. Bindels, J. Bijvoet, G. W. Rathenau, *Physica 26, 13,(1960).*
- [46] P. R. Moharkar, S. R. Gawali, K. G. Rewatkar, V. M. Nanoti., *ICBEST 2012 Proceedings published by International Journal of Computer Applications® (IJCA).*
- [47] M. K. Rendale ,S. D. Kulkarni and V. Puri., *Int. Journal Microelctron-ics 26, 43, (2009).*
- [48] L. Patron , I. Mindru and G. Marinescu , Dekker., *Encyclo-pedia of Nanoscience & Nanotechnology, second edition. (2009).*

